Scientia Iranica, Vol. 7, No. 1, pp 25-31

SCIENTIA
IRANICA

Guard-Ring Effects on Capacitive Transducer Systems

H. Golnabi[1]

In this paper, implementing a guard-ring electrode in a capacitive transducer system is described. The performance of the transducers with and without a guard-ring in terms of output linearity and dynamic range is investigated and deviations from the expected theoretical results are reported. The two-terminal capacitors perform well only for a small gap distance in the range of 2-3 mm while the three-terminal sensor (50 mm diameter) demonstrates a very good performance for a wide range of 0.5-5 mm. For a gap distance of 3 mm, the slope deviation for the sensors without a guard-ring is in the range of 15%-29%, whereas for the system with a guard-ring is only 6%, which clearly shows the range effectiveness of the third electrode for such transducer systems.

INTRODUCTION

The field of industry has always been dependent on measuring instruments and for this reason the technology behind sensors and transducers has a long tradition. Capacitive transducers are being used in many industrial applications to control processes and machine diagnoses. Various parameters such as distance, pressure, torque, etc. can be sensed through capacitive transducer systems [1,2]. However, several problems including stray capacitance, baseline drift, stability and sensitivity have motivated the development of new transducers and measuring systems. In this respect, the effects of a guard-ring electrode on the operation of a capacitive transducer system have been considered in this study.

A new capacitive-to-phase conversion technique for measuring very small capacitance changes has been recently reported [3-5]. Based on this method, a prototype version is constructed and the ability of the new readout circuit with a capacitive transducer is demonstrated. In this work, implementation of the new measuring technique provides powerful means for recording very small displacements or corresponding capacitance changes.

The effects of a guard-ring electrode on the performance of capacitive sensor systems are explored. Special attention is paid, in particular, to the linearity of the output line and the effective dynamic range of each system. The experimental results for both sensors (with and without a guard-ring) are presented. The resulting differences in their operations provide an insight into the performance and application of such transducer systems.

1. *Institute of Water and Energy, Sharif University of Technology, P.O. Box 11365-8639, Tehran, I.R. Iran.*

THEORETICAL ANALYSIS

Guard-Ring Effect

The capacity of a parallel-plate capacitor can be obtained from:

$$C = \varepsilon A/d, \tag{1}$$

where ε is permitivity of the dielectric medium between the plates, A is electrode area and d is gap distance between the electrodes. However, Equation 1 is only valid when $A >> d$.

Several problems, such as edge effect, can cause deviations in the actual capacity from the one obtained in Equation 1. For this reason, various attempts have been made to design different transducers in order to reduce these effects [6]. One simple remedy has been the use of a Kelvin guard-ring [7] in which the main inner electrode is shielded by a grounded guard-ring. For this geometry, when the gap distance between the main electrodes (d) is much smaller than the difference between the radii of the outer and inner electrodes, one can write:

$$C = \varepsilon A_e/d, \tag{2}$$

in which A_e is the effective area of the capacitor, considered to be:

$$A_e = \pi R_e^2 = \pi(R + \delta/2)^2, \tag{3}$$

where R is the radius of the inner electrode and δ is the thickness of the dielectric material separating the main inner electrode and the guard-ring. So far, the effect of a guard-ring on the capacity of a transducer has been considered, but in the next section its role in the final measured values is discussed.

Capacitance-to-Phase Conversion

The measuring method presented here requires two phase balanced signals as shown in Figure 1. A simple circuit was proposed for producing two 180 degree out-of-phase signals in the previous report [8], which is employed in the measuring circuit. The two AC signals are produced from a single sinusoidal input signal by using two matched op-amps. The phase accuracy of the circuit was investigated in that report for 0-4 MHz frequency range. At low frequencies, the phase error for producing such signals is negligible. However, at high frequencies, the effects of non-ideal circuit elements cause deterioration from the ideal response.

The calculated phase error at 2 MHz was found to be about 0.5 degrees, while the measured value was about 1 degree. At operating frequency of 10 kHz, used in this measuring circuit, the phase deviation was found to be less than 0.5 degrees. The phase shift, ψ, is produced by using R_1 and C_1, as shown in Figure 1c. The ψ value is defined by $\tan^{-1}(R_1 C_1 \omega)$ and, for $R_1 = 2k\Omega$, $C_1 = 10$ nF and $f = 1$ kHz, is about 7.15 degrees. At the end, two signals defined as $A\sin(\omega t)$ and $B\sin(\omega t + \pi - \psi)$ are obtained, where A and B are the amplitudes (about 5V).

Even though the ψ value is fixed by $R_1 C_1 \omega$, in practice, there may be some drift in ψ as a result of minor variations in these parameters. Therefore, selection of proper components and a well-defined oscillation frequency are the key points in successful operation of such circuits.

The capacitance-to-phase conversion principle is simply displayed in Figure 1a. Two input signals defined by $A\sin(\omega t)$ and $-B\sin(\omega t - \psi)$, are fed into an op-amp and the capacitance change is measured by the ratio of the in-phase and the quadra-phase output amplitudes. The output of op-amp, V_0, is given by:

$$V_0 = \frac{AC_x \sin(\omega t) - BC_0 \sin(\omega t - \psi)}{C_x + C_0 + C_T}, \tag{4}$$

where C_0 and C_T are shown in Figure 1b. Now, if the in-phase amplitude, V_c, is compared with quadra-phase amplitude, V_s, then, it can be written that:

$$V_c = \frac{AC_x - BC_0 \cos\psi}{C_x + C_0 + C_T}, \tag{5}$$

$$V_s = \frac{BC_0 \sin\psi}{C_x + C_0 + C_T}, \tag{6}$$

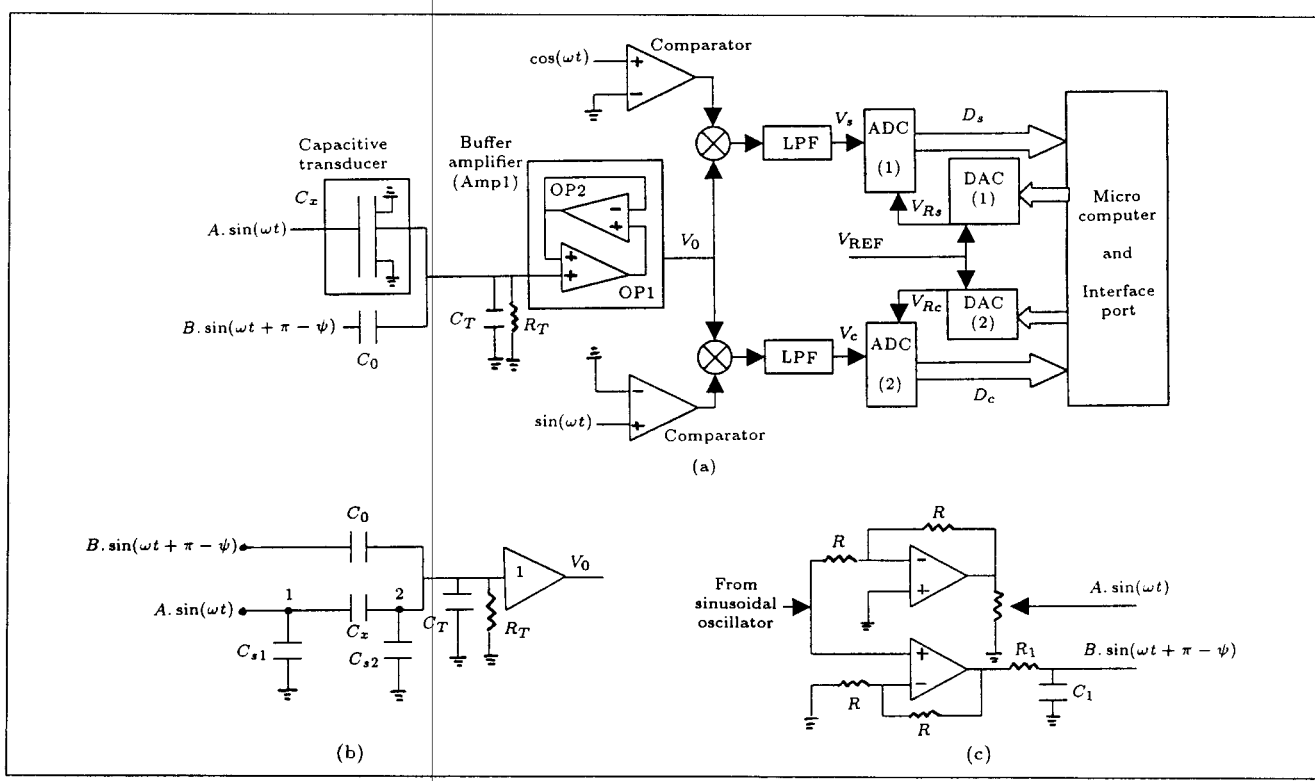

Figure 1. (a) Block diagram of the readout circuit and monitoring system. (b) Circuit for measuring the effect of a constant stray capacitance C_{s1} or C_{s2}. (c) Circuit to produce phase shift, ψ.

and by dividing two amplitudes:

$$V_{\text{out}} = \frac{V_c}{V_s} = \frac{AC_x - BC_0 \cos\psi}{BC_0 \sin\psi} \ . \tag{7}$$

The measuring principle is to compare the in-phase amplitude with the quadra-phase amplitude, which is affected by A, B, C_x, C_0 and ψ, as can be seen in Equation 7. This means that, in general, Equation 7 is not linear in C_x unless other parameters remain fixed and stable during the measurements.

The value of C_x, in general, can be the sum of the different terms such as:

$$C_x = C_{x_0} + C_{x_1} + C_{st}, \tag{8}$$

where C_{x_0} is the capacity of the transducer at initial gap distance X_0, C_{x_1} is the capacitance caused by a displacement X_1 from X_0 and C_{st} is the total stray capacitance affecting the transducer. By substituting C_x from Equation 8 into Equation 7:

$$V_{\text{out}} = \frac{AC_{x_0}}{C_0 B \sin\psi} + \frac{AC_{x_1}}{C_0 B \sin\psi} - \cot\psi + \frac{AC_{st}}{C_0 B \sin\psi}. \tag{9}$$

Now, if one neglects the effect of stray capacitance in the last term of Equation 9 and by carefully adjusting the circuit to compensate the standing value, C_{x_0}, then:

$$AC_{x_0} = BC_0 \cos\psi, \tag{10}$$

and the following equation holds for the detected output:

$$\frac{V_c}{V_s} = \frac{C_{x_1}}{C_{x_0}} \cot\psi \ . \tag{11}$$

If the normalized capacitance ratio C_{x_1}/C_{x_0} is considered, then it can be written that:

$$\frac{C_{x_1}}{C_{x_0}} = \frac{V_c}{V_s} \tan\psi, \tag{12}$$

and the normalized digitized output signal becomes:

$$D_{\text{out}} = \frac{C_{x_1}}{C_{x_0}} = \frac{D_c}{D_s} \frac{\tan\psi}{(V_{Rs}/V_{Rc})} \ , \tag{13}$$

where V_{Rs} and V_{Rc} are two reference voltages for the DACs; D_s and D_c are the digitized output of the corresponding ADCs which are shown in Figure 1a.

In this measuring method, any changes in the value of C_{x_1} can be detected. By exchanging the position of C_{x_0} and C_0 in the circuit (see Figure 1), the output line from Equation 13 becomes:

$$D_{\text{out}} = \frac{X_1}{X_0} = \frac{D_c}{D_s} \frac{N_c}{N_s} \tan\psi, \tag{14}$$

where N_c and N_s are the digital input numbers of two DACs (N_c/N_s is equal to V_{Rc}/V_{Rs}) and X_0 is the distance at which the zero adjustment is made. A condition that Equation 10 is satisfied and the effects of A, B and C_0 on measurement values are eliminated. Here, $1/X_0$ defines the slope of the output line for the sensor.

To derive Equation 14, it was assumed that the capacitive transducer is well-guarded and C_x, according to Equation 2, is given by:

$$C_x = \frac{\varepsilon A_e}{X_0 + X_1}, \tag{15}$$

while for a general case of a transducer without a guard-ring, it must be written as:

$$C_x = \frac{\varepsilon A_e}{X_0 + X_1} + C_{st}(X_0, X_1), \tag{16}$$

where C_{st} exists and may vary with parameters X_0 and X_1.

In a case where there is a variable stray capacitance on the transducer, the new C_x should be substituted in Equation 4 which changes the obtained output line of Equation 14. For a guard-ring capacitor, it was found that constant stray capacitance only has a small effect on the readout which was less than 0.1% for adding a stray capacitance of $C_{s1} = C_{s2} = 180$ pF (see Figure 1b). However, the slope of the calibration line remained unchanged.

For a transducer with some stray capacitance, two major effects can cause deviation in the derived formulas. First, zero adjustment is only valid for a case in which stray capacitance is neglected. The second and perhaps the most important case is when C_{st} varies with X_0 and X_1 values which has effect on zero adjustment and also a considerable effect on output line slope.

EXPERIMENTAL METHOD

The block diagram of the apparatus for data collection is presented in Figure 2. The main components are: a capacitive sensor, a stepper motor, a drive circuit, a capacitance measuring circuit and a P.C., which is interfaced with the readout and also controls the stepper drive via an interface card. In this arrangement, one of the capacitor plates is fixed in position while the other plate is moved in a parallel way, via a coupler, which connects the motor shaft to the plate holder. It is, therefore, possible to scan the air-gap distance precisely by the computer-controlled stepping motor drive system.

The schematical cross-section of the capacitive transducer used in this study is represented in Figure 3. In designing this capacitive transducer, care was taken

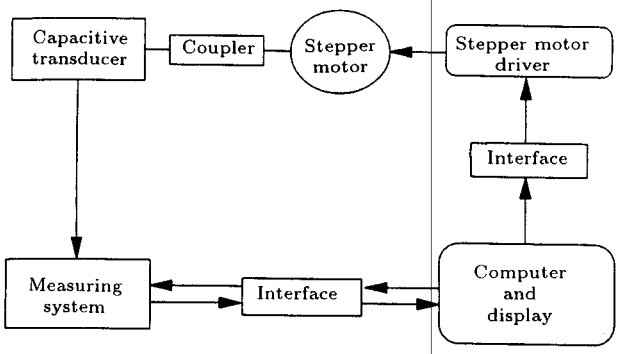

Figure 2. Block diagram of the apparatus used in this study.

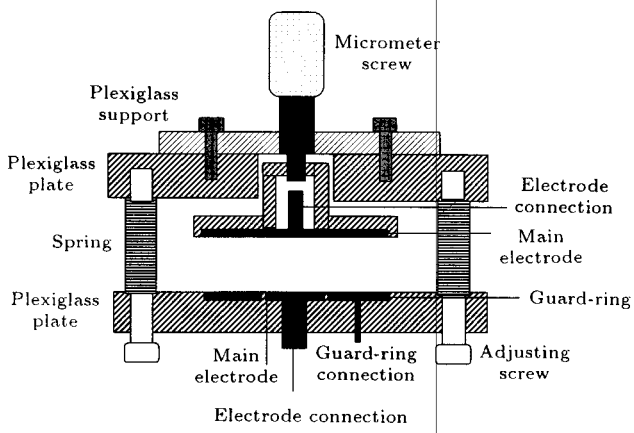

Figure 3. Schematical cross-section of the capacitive transducer.

to minimize the nonlinearity errors by careful design of guard electrodes and gaps. Parameters such as sensitivity to electrode distance variation, lateral displacement as well as tilting and bending of electrodes were considered in the transducer construction. The gap conditions such as air humidity and temperature variation can be some other sources of nonlinearity in the transducer performance. Besides transducer nonlinearity, some errors may be caused by the nonlinearities of the scanning drive and the measuring circuit.

The stepper motor coupling arrangement provides a smooth and precise movement of the main electrode for a range of 0.5 to 7 mm without any stalling problem or backlash. To show the result of this scanning system, the hysteresis curve for the transducer system driven by a stepper motor is presented in Figure 4. As can be seen in this figure, for an initial gap distance of $X_0 = 3.5$ mm and a possible scanning range of 1 mm, there is little hysteresis effect for the reported transducers.

The special design of the transducer permits the easy exchange of the lower electrode as can be seen in Figure 3. This feature makes it possible to use the system in either two- or three-terminal configuration. In this experiment, two electrode plates without a guard-ring and one with a guard-ring have been constructed. The upper electrode was common

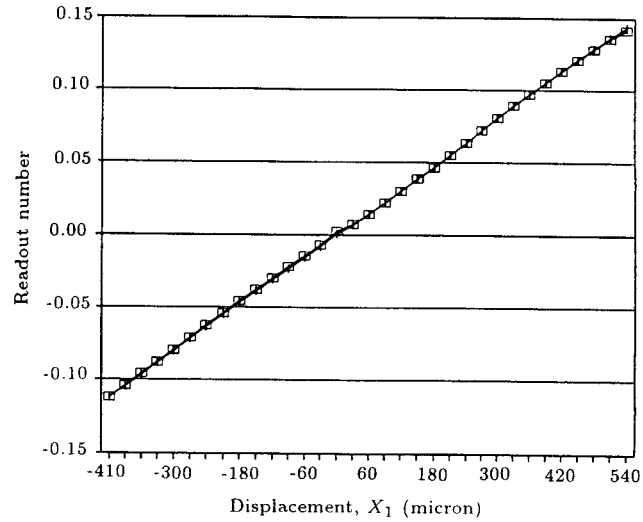

Figure 4. Hysteresis curve of the reported transducer system.

in the three cases, having a diameter of 50 mm. For the guard ring electrode, the inner main electrode has a diameter of 25 mm and the guard-ring has an inner diameter of 26 mm ($\delta = 1$ mm) and an outer diameter of 50 mm. The nominal capacity of this transducer at $X_0 = 1$ mm is about 4.55 pF.

For the case of no guard-ring, two plates with diameters of 25 and 50 mm were used in turn. The capacitive transducer with the smaller plate in place provides a nominal capacitance of about 4.34 pF while the larger one has a capacitance of 17.36 pF at a gap distance of $X_0 = 1$ mm.

RESULTS

In the first experiment, the operation of the sensors at different gap distances ranging from 0.5 mm to 7 mm was investigated. The results of this study for the gap distance of 1 mm are presented in Figure 5. To compare the responses of the three systems, the deviations of the experimental results from those expected from Equation 14 are presented. As can be seen in Figure 5, the sensor with a guard-ring marked A shows the lowest deviation for the experimented 85 μm scanning range.

However, the curve marked as B in Figure 5 corresponds to the behavior of the transducer without a guard-ring, which has similar plates. In this case, there is a higher deviation from the predicted results of Equation 14 which indicates that some kind of stray capacitance is affecting the transducer. Consequently, to explore the stray effects, similar experiments were performed on the transducer with a smaller lower plate. The considerable difference between its performance (curve C) and the others indicated that at this range, there is a considerable stray capacitance due to the edge effect as well as some effects resulting from the backside of the lower plate.

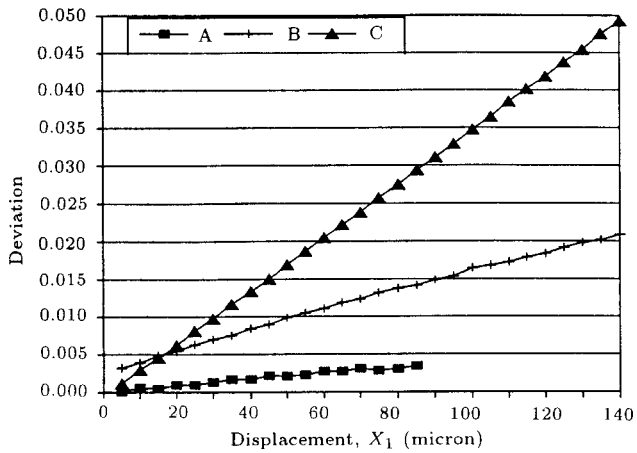

Figure 5. Deviation of the sensors' outputs from the expected results of Equation 14 at $X_0 = 1$ mm. (A) transducer with a guard-ring, (B) transducer without a guard-ring and similar plates and (C) transducer without a guard-ring and unequal plates.

In another experiment, the stray effects at higher gap distances were explored. For this purpose, the sensor performances at a gap distance of 6 mm have been shown in Figure 6. By comparing the results of Figures 5 and 6, two major effects can be noticed. First, the second sensor without a guard-ring (curve B) has stray capacitance which is mainly due to edge effect and is less sensitive to increase in the gap distance. Second, for the sensor without a guard-ring and a smaller lower plate, deviation from the predicted results becomes smaller at higher X_0 values (as discussed in the theoretical analysis) which is an indication that the stray capacitance for this transducer is inversely related to the gap distance X_0. As the gap distance is increased, there seems to be a better agreement with results from the guard-ring transducer and also with the theoretical expectations.

A series of experiments were performed at different gap distances in order to check the linearity of the transducers. For this purpose, the performance of each transducer was studied at different X_0 values. The nonlinearity factor defined here is the maximum difference between the experimental value minus the best least-squares line fitted to the experimental data points divided by the full output range [9]. The results of this study are presented in Figure 7. As can be seen in this figure, the sensor with a guard-ring has the best linearity for the experimental range of 0.5 to 7 mm.

The nonlinearity factor for the transducer without a guard-ring and with similar big plates is higher than the one with a smaller plate as can be noticed in Figure 7. The reason for this behavior might be the parallelizm of the big plates and some non-uniformity in the gap distance. Due to higher uniformity in the third sensor, a better linearity can be observed. However, the nonlinearity of the three transducers, in particular the one with a guard-ring, is remarkable for this range of operation. Actually this is one of the strongest advantages of such a capacitive transducer and readout system.

The crucial point regarding the performance of this transducer is the calibration line for the system which was studied at different gap distance values and zero settings at each X_0 value. Then, by using a least-squares program the best line with the corresponding slope was determined. The final results for a series of experiments are shown in Figure 8. The slope deviations from the best line shown in Figure 8 reveal three major points. First, the transducer with a guard-ring shows less deviation from the expected theoretical line of Equation 14. Second, the deviations observed for

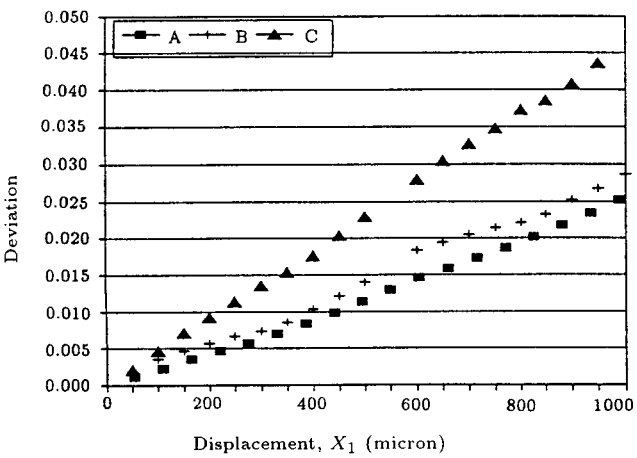

Figure 6. Deviation of the sensors' outputs from the theory at $X_0 = 6$ mm. (A) with a guard-ring, (B) no guard-ring and similar plates and (C) without a guard-ring and unequal plates.

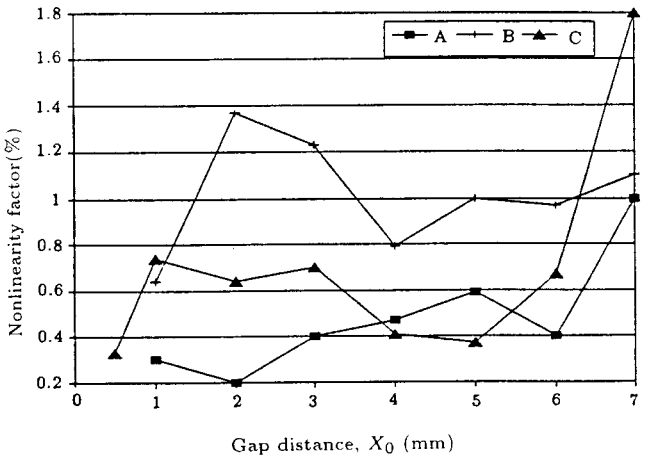

Figure 7. Comparison of the nonlinearity factor for three transducers as a function of initial gap distance X_0 . (A) with a guard-ring, (B) without a guard-ring and similar big plates and (C) no guard-ring and unequal plates.

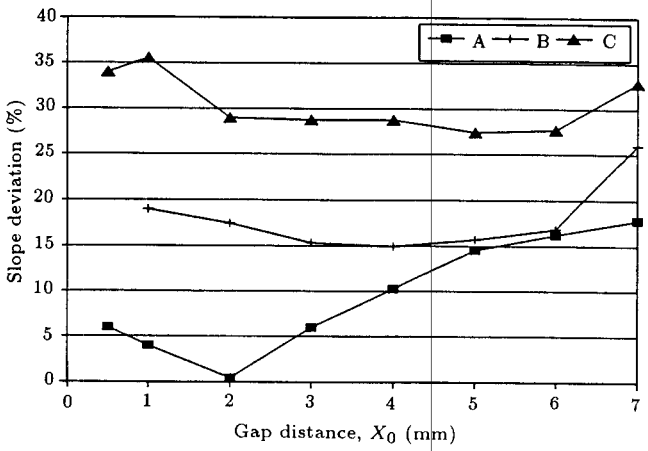

Figure 8. Slope deviations from the expected theory of Equation 14 for three transducers at different gap distances and different zero settings. (A) three-terminal with a guard-ring, (B) two-terminal with equal big plates, and (C) two-terminal with unequal plates.

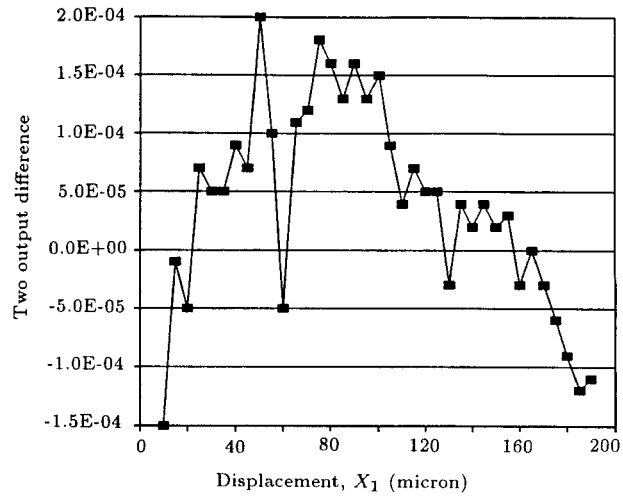

Figure 9. Measured differences in the two outputs to show the repeatability of the experiments (transducer without a guard-ring at $X_0 = 1$ mm).

the sensors without guard-rings demonstrate variations with X_0 values which suggest that the stray capacitance is depending on this parameter.

Third, a better agreement of the three responses at higher X_0 values prevails that the stray capacitance for the transducers without a guard-ring is inversely dependent on this parameter. For the transducer marked with the response curve B, there seems to be only stray capacitance due to edge effect which is more or less constant for different X_0 values. However, for the transducer C, there are two sources of stray capacitance, one resulting from edge effect and the other one because of the backside of the lower plate.

At smaller gap distances, the backside effect is dominating while at higher X_0 values, the edge effect is more pronounced. Considering the results of Figures 7 and 8, one may conclude that the transducers without guard-ring protection are performing relatively well for only a gap distance of 2-3 mm while the one with the guard-ring has a very good performance for a long range of 0.5-5 mm. In particular, the range of 0.5 to 4 mm, which demonstrates satisfactory linearity and a calibration line is in close agreement with the theory.

The effects of the guard-ring on the other parameters of the transducer, such as its stability and repeatability, were also investigated. The stability of the systems without a guard-ring is as good as the one with the guard-ring electrode. The repeatability of the transducer without a guard-ring is shown in Figure 9, which is nearly the same as the one with a guard-ring.

CONCLUSIONS

Operations of capacitive transducers with and without guard-ring electrodes have been described in this paper. Except for one of the electrodes, the rest of the apparatus remains unchanged for each experiment; therefore, this method provides a very accurate way to explore the effects of a guard-ring electrode on the results. The performance of a transducer with a guard-ring and two different transducers without guard-rings in terms of linearity, stability, repeatability, output line and dynamic range has been investigated.

By comparing the experimental results of the two- and three-terminal transducers and also the related theories, major conclusions are as follows:

1. The stability and the repeatability of the two-terminal transducers are as good as the sensor with a guard-ring and all the sensor systems show a little hysteresis effect in their operations.
2. The linearity of the transducers without a guard-ring electrode is comparable with the one with the guard-ring electrode; although the two-terminal capacitive transducer with larger plates illustrates a higher nonlinearity factor in its operation.
3. The major difference between the performances of the two- and three-terminal transducers is due to their slope deviation, which is the most important parameter in this measuring instrument.

The two-terminal transducer with unequal electrode plates has the worst slope deviation from the expected result after which the other two-terminal transducer shows an acceptable operation only for a very small dynamic range. Overall performance of these sensors demonstrates that because of edge effects and other effects resulting from backside plate, these devices are not suitable for gap distances less than 2 mm. On the other hand, other parameters limit their operation to a range of 2-3 mm. As expected, the transducer with a guard-ring shows a very good linearity and output line for a long operation range of 0.5 to 5 mm, which makes it a sensitive tool

for measuring very small capacitance or displacement changes. Because of the high sensitivity of the readout system, the reported design provides good means for detecting any small stray capacitance interfering with a capacitive transducer [10].

ACKNOWLEDGMENTS

This research project was supported in part by Sharif University of Technology Research Organization. The author is, therefore, grateful for the grant provided by the Research Council. The author would also like to thank A. Ashrafi for the assistance given during the experimental measurements. He is also grateful to Mrs. Tavakoli for the preparation of this manuscript.

REFERENCES

1. Wolffenbuttel, R.F., Mahmoud, K.M. and Regtien, P.P.L. "Compliant capacitive wrist sensor for use in industrial robots", *IEEE Trans. Instrum. Meas.*, **IM-39**, pp 991-997 (1990).
2. Lee, Y.S. and Wise, K.D. "A batch - fabricated silicon capacitive pressure transducer", *IEEE Trans Electron Devices*, **29**, pp 42-47 (1982).
3. Wolffenbuttel, R.F. and Regtien, P.P.L. "Capacitive-to-phase angle conversion for the detection of extremely small capacities", *IEEE Trans. Instrum. Meas.*, **IM-36**, pp 868-872 (1987).
4. Kung, J.T., Lee, H.S. and Howe, R.T. "A digital readout technique for capacitive sensor applications", *IEEE J. Solid State Circuits*, **23**, pp 972-977 (1988).
5. Van der Goes, F.M.L. and Meijer, G.C.M. "A novel low-cost capacitive-sensor interface", *IEEE Trans. on Instrumentation and Measurement*, **IM-45**, pp 536-540 (1996).
6. Heerens, W.C and Vermeulen, F.C. "Capacitance of Kelvin guard-ring capacitors with modified edge geometry", *J. Appl. Phys.*, **46**, pp 2486-2490 (1975).
7. Heerens, W.C. "Multi-terminal capacitor sensors", *J. Phys. E: Sci. Instrum.*, **15**, pp 137-141 (1982).
8. Golnabi, H. and Ashrafi, A. "Producing 180° out-of-phase signals from a sinusoidal waveform input", *IEEE Trans. Instrum. Meas.*, **IM-45**, pp 312-314 (1996).
9. Jacob, J.M., *Industrial Control Electronics*, Prentice-Hall Inc., New Jersey, Chap. 3, pp 72-75 (1989).
10. Huang, S., Green, P.G., Plaskowski, R. and Beck, M.S. "A high frequency stray-immune capacitance transducer based on the charge transfer principle", *IEEE Trans. Instrum. Meas.*, **IM-37**, pp 368-373 (1988).